Journal of Advanced Ceramics
2013, 2(1): 55–62
DOI: 10.1007/s40145-013-0042-4 ISSN 2226-4108

Research Article

Characterization of yttria-stabilized zirconia films deposited by dip-coating on $La_{0.7}Sr_{0.3}MnO_3$ substrate: Influence of synthesis parameters

Jacqueline C. MARRERO[a], Nielson F. P. RIBEIRO[a], Célia F. MALFATTI[b], Mariana M. V. M. SOUZA[a,*]

[a]*Escola de Química—Universidade Federal do Rio de Janeiro* (*UFRJ*), *Centro de Tecnologia*, *Bloco E*, *sala 206*, *Ilha do Fundão*, *CEP 21941-909*, *Rio de Janeiro*, *RJ*, *Brazil*
[b]*Departamento de Metalurgia*, *Universidade Federal do Rio Grande do Sul* (*UFRGS*), *Campus do Vale*, *Setor 4*, *Prédio 75*, *Sala 234*, *CEP 91501-970*, *Porto Alegre*, *RS*, *Brazil*

Received: December 29, 2012; Revised: January 24, 2013; Accepted: January 26, 2013

Abstract: Yttria-stabilized zirconia (YSZ, ZrO_2–8%Y_2O_3) films were deposited onto lanthanum strontium manganite (LSM, $La_{0.7}Sr_{0.3}MnO_3$) substrates using dip-coating process aiming for the application in solid oxide fuel cells (SOFCs). YSZ precursor was prepared by sol–gel method; three values of the organic/inorganic concentration ratio (1, 3 and 5) were utilized and the sol viscosity was adjusted (60 mPa·s and 100 mPa·s) before deposition on the substrate. The influence of these synthesis parameters on the structure and morphology of the deposited films was examined by X-ray diffraction (XRD) and scanning electron microscopy (SEM). The films showed characteristic peaks of LSM, YSZ (with cubic structure) and secondary phases of $SrZrO_3$ and La_2O_3. Depending on the synthesis conditions, crack-free, homogeneous and well adhered films were obtained, with thickness of 11–24 μm.

Keywords: YSZ; films; LSM; sol–gel; dip-coating

1 Introduction

Solid oxide fuel cells (SOFCs) have grown in recognition as a viable high temperature fuel cell technology. SOFC is a complete solid-state device that uses an oxide ion-conducting ceramic material as electrolyte and operates in the temperature range of 800–1000 ℃. When compared with conventional methods of power generation, SOFCs have many advantages, such as higher energy conversion efficiency which can reach up to 65%, easy modular construction, a wide range of fuel possibilities, potential for cogeneration, and life expectancy of more than 40 000 h [1,2]. The current focuses in SOFCs research are material development and reduced-temperature operation.

Yttria-stabilized zirconia (YSZ) is a commonly used electrolyte material in SOFCs due to its pure ionic conductivity, long-term stability, good chemical compatibility with other cell components and excellent mechanical properties [3]. On the other hand, lanthanum strontium manganite (LSM) is the most widely used cathode material due to its high electrical

* Corresponding author.
E-mail: mmattos@eq.ufrj.br

conductivity in an oxidizing atmosphere, thermal and chemical phase stability, and relatively good compatibility with YSZ electrolyte [3,4]. One approach to overcome the resistivity of the electrolyte at operation temperatures below 800 ℃ is to reduce the thickness of the electrolyte. Thus it is desirable to fabricate cathode-supported cells with electrolyte films of only a few microns thick.

Various physical or chemical processes have been used for the preparation of YSZ thin films, such as electrochemical vapor deposition (EVD), chemical vapor deposition (CVD), physical vapor deposition (PVD), electrophoretic deposition (EPD), thermal spraying, colloidal deposition, sputtering, tape calendaring, sol–gel method, and dip-coating [2,5]. Among these methods, the sol–gel method provides several advantages: the microstructure and composition can be easily controlled; low-temperature processing is possible; the adhesion on the substrate is strong [6,7]. Deposition of thin films by dip-coating is considered to be simple and cost effective, producing uniform coating with large areas and controllable film thickness and density [8].

The composition of the dip-coating slurry and its physico-chemical properties have a significant influence on the quality of YSZ films. Wang *et al*. [8] reported the preparation of YSZ films on the porous NiO–YSZ substrate, using dip-coating process. They developed a dip-coating slurry with YSZ powders dispersed in triethanolamine (TEA), ball-milled with binders and plasticizers. A two-layer film with thickness of 16 μm was determined to be homogeneous, crack-free and well-adherent to the substrate. Lenormand *et al*. [9] also reported the preparation of YSZ films by dip-coating on NiO–YSZ substrate. A suspension of YSZ powders in a MEK–EtOH (methylethylketone–ethanol) azeotropic solvent was added to a polymeric matrix obtained by the reaction between hexamethylentetramin (HMTA) and acetilacetone. Continuous and homogeneous films with 20 μm thickness were obtained, which is in good agreement with the requirements for SOFC electrolyte working at 700 ℃. Gaudon *et al*. [10] used a similar procedure to deposit YSZ films on NiO–YSZ substrate, with thickness varying between 8 μm and 80 μm. On the other hand, Lenormand *et al*. [11] studied the preparation of $La_{0.8}Sr_{0.2}Mn_{1-y}Fe_yO_{3+\delta}$ ($y = 0$, 0.2, 0.5, 0.8 and 1) films on YSZ substrate by dip-coating, using metal salt precursors and organic compounds (HMTA, acetilacetone and acetic acid) for various R (organic/inorganic concentration ratio) values. The authors obtained continuous, homogeneous and crack-free thin films.

In the present study, the preparation of YSZ films on the porous LSM substrate using sol–gel/dip-coating process has been investigated. The methodology was adapted from Lenormand *et al*. [9,11]. The main objective of the present study is to characterize YSZ films prepared by using different synthesis parameters (sol viscosity and organic/metal salt concentration ratio).

2 Experiment

2.1 Substrate preparation

$La_{0.7}Sr_{0.3}MnO_3$ (LSM) powders were prepared by the combustion method using metal nitrates and urea, followed by calcination in air (60 ml/min) at 10 ℃/min up to 750 ℃ for 10 h. The detailed experiments have been reported in our previous work [12]. The powders were then pressed into pellets (13 mm diameter and 2 mm thickness) under uniaxial pressure of 200 MPa, and subsequently sintered with a heating rate of 10 ℃/min up to 1300 ℃ for 2 h. After that, the surface of the fired pellets was polished with SiC sandpaper (4000 mesh). The pellet porosity is 39%, measured by Archimedes method.

2.2 Preparation of YSZ sol–gel

YSZ (ZrO_2–8%Y_2O_3) film precursors were prepared by a polymeric sol–gel process. The solution of metal salts was prepared from $ZrO(NO_3)_2$ and $YCl_3{\cdot}6H_2O$ with concentration of $C_s = 1$ mol/L. An organic solution consisting of complexing and polymeric agents (hexamethylentetramin (HMTA–$C_6H_{12}N_4$), acetylacetone (acac–$C_5H_8O_2$) and acetic acid (a.a.–$C_2H_4O_2$)), with C_o concentration, was added to the metal salt solution to promote polyesterification and polycondensation reactions [11]. R, defined as the ratio of organic compound concentration (C_o) to metal salt concentration (C_s), were 1, 3 and 5. The obtained sol was refluxed at 80 ℃ on a hot plate until the desired viscosity (60 mPa·s or 100 mPa·s) was reached, forming the YSZ gel.

The viscosity of YSZ sol precursor was measured by a function of relative volume reduction, defined as $[(V_{\text{initial}} - V_{\text{final}})/V_{\text{initial}}] \times 100$, which is a consequence of solvent evaporation during heating. Sol viscosity was

measured with a LDVE II+ Brookfield Viscometer at 25 ℃.

2.3 Deposition of YSZ films

The as-obtained YSZ gel was deposited on LSM substrate at room temperature by dip-coating technique. The withdrawal speed was 50 mm/min and the time of deposition was 40 s. The films were dried with a heating rate of 2 ℃/min up to 70 ℃ for 30 min and then sintered with a heating rate of 2 ℃/min up to 1300 ℃ for 2 h.

2.4 Characterization

The crystalline structure of the films was analyzed by X-ray diffraction (XRD) using a Rigaku Miniflex II equipment with Cu Kα radiation and 2θ range from 10° to 90°. The XRD patterns were analyzed using JCPDS (Joint Committee on Powder Diffraction Standards) database of crystal structures. The crystallite size (D_{XRD}) and microstrain (ε) were calculated using Eq. (1) [13]:

$$\beta\cos\theta / \lambda = 1 / D_{\mathrm{XRD}} + 4\varepsilon\sin\theta / \lambda \quad (1)$$

where λ is the X-ray wavelength (0.154 nm), θ is Bragg diffraction angle and β is the FWHM (full width at half maximum) of the peak.

Scanning electron microscopy (SEM) was carried out to characterize both morphology and microstructure of YSZ films, using a HITACHI TM-1000 Microscopy with energy dispersive spectrometry (EDS).

3 Results and discussion

3.1 LSM substrate

The XRD pattern of the LSM pellets sintered at 1300 ℃ is shown in Fig. 1. The peaks indicate the formation of only LSM perovskite phase (JCPDS 401100). The crystallite size and microstrain, calculated from the XRD data, were 21.5 nm and 0.49%, respectively.

Figure 2 shows the SEM micrographs of the surface of LSM substrate after calcination, sintering and polishing with sandpaper. The calcined powders showed the agglomeration of the particles leaving a spongy structure while the sintered substrate had lower porosity. After the polishing process there was a significant improvement in the substrate surface, reducing the porosity and leaving a more homogeneous surface.

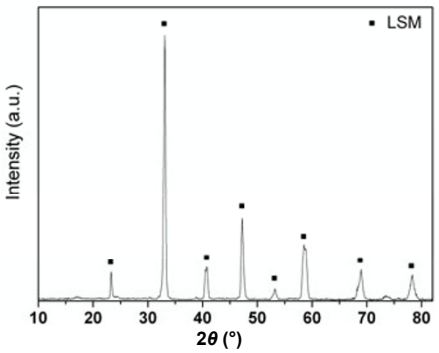

Fig. 1 XRD pattern of the LSM substrate sintered at 1300 ℃ for 2 h.

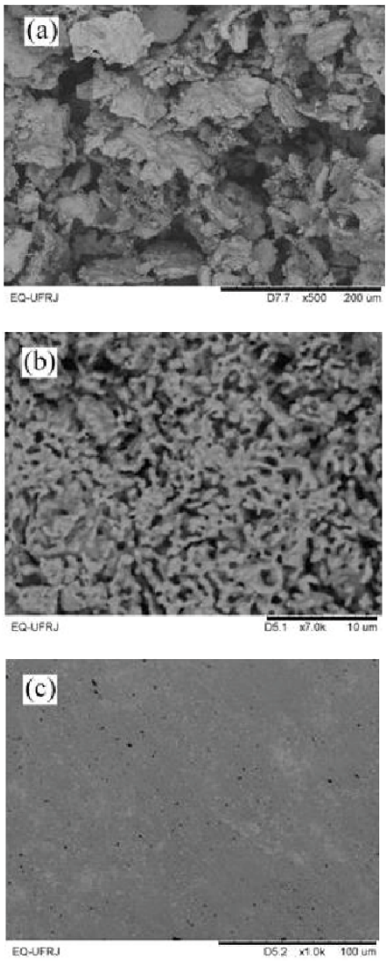

Fig. 2 SEM micrographs of LSM substrate: (a) calcined, (b) sintered and (c) sanded.

3.2 YSZ sol viscosity

It is important to control the viscosity of the YSZ sol

precursor to yield continuous and crack-free films, because if the sol viscosity is too low, a discontinuous film may be formed, while if the sol viscosity is too high, cracks may appear in the thin film [14].

Figure 3 shows the viscosity of the YSZ sol versus volume reduction during heating for different R values ($R=1$, 3 and 5). The viscosity increases with volume reduction according to the organic content of the YSZ sol. The YSZ sol viscosity firstly remains almost constant for small reductions in volume, and then sharply increases with volume reduction due to polimerization of HMTA. The polimerization is faster for higher R values. Similar results were obtained by Lenormand *et al*. [11] for $La_{0.8}Sr_{0.2}Mn_{1-y}Fe_yO_3$ sols with $R=5.3$, 10.5 and 15.

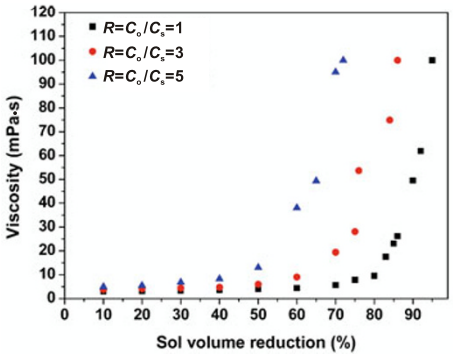

Fig. 3 Evaluation of YSZ sol viscosity as a function of volume reduction for $R=C_o/C_s=1$, 3 and 5.

3.3 Phases of the YSZ films

X-ray diffraction patterns of YSZ films deposited on LSM substrate are presented in Fig. 4 for various R values ($R=1$, 3 and 5) and two viscosities (60 mPa·s and 100 mPa·s). XRD patterns of the films are similar for all values of R, with better definition of YSZ peaks for the higher viscosity (100 mPa·s).

The XRD patterns of the films showed the YSZ cubic phase (JCPDS 301468), perovskite phase (attributed to LSM substrate) and diffraction peaks at 30.7°, 44.2° and 54.9° correspondent to the formation of $SrZrO_3$ (SZ) phase (JCPDS 44161). Small peaks at 21°, 28.1° and 45° may be attributed to La_2O_3 (JCPDS 22641) formed during severe heat treatment of LSM [15]. The formation of these secondary phases is more pronounced for the samples prepared with lower viscosity.

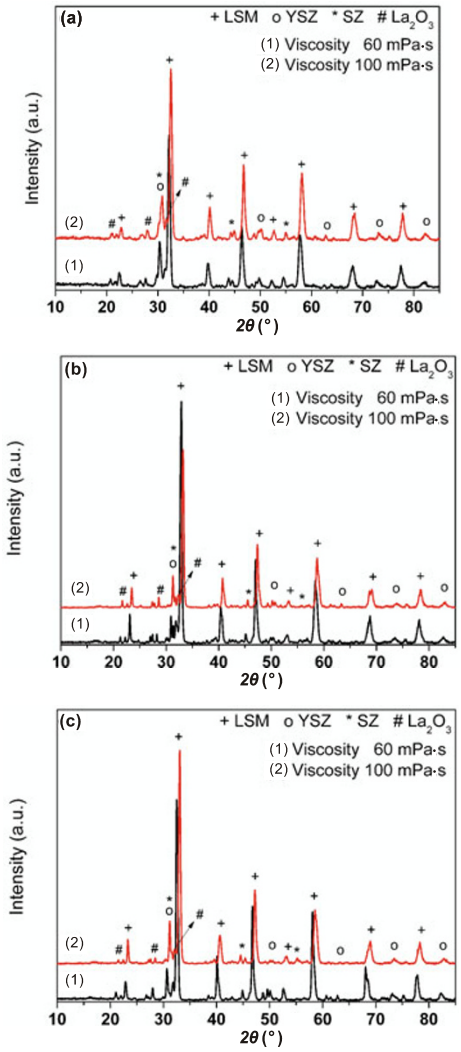

Fig. 4 XRD patterns of YSZ films prepared with (a) $R=1$, (b) $R=3$ and (c) $R=5$, and sintered at 1300 ℃ for 2 h.

It is well known that LSM can react with YSZ at high temperatures to form insulating phases of $La_2Zr_2O_7$ (LZ) and $SrZrO_3$ (SZ) [3,16,17]. Both phases weaken the electrical contact of cathode/electrolyte because the conductivity of these zirconates is at least 2–3 orders of magnitude lower than that of YSZ electrolyte [18]. However, LZ and SZ phases formed at the interface will probably disappear from the three-phase boundaries on cathodic polarization because of the shift of the oxygen potential to the more reducing side [3]. Yang *et al.* [2] have observed that LZ phase appeared at the interface between YSZ film and LSM only after 52 h of sintering at 1400 ℃. Lee *et al*. [5] reported that films sintered at 1300 ℃ for 2 h showed only cubic YSZ phase; on the other hand, as the sintering temperature increased to 1400 ℃, a

second phase of LZ was formed. In these two works, YSZ films were deposited on LSM using EPD.

The presence of SZ phase can be due to the high sintering temperature. In fact, Brant *et al*. [19] observed the formation of SZ at the interface between YSZ and porous LSM after annealing over 1200 ℃. According to van Roosmalen and Cordfunke [20], the formation of SZ from $La_{0.7}Sr_{0.3}MnO_3$ and ZrO_2 is estimated to start at 1247 ℃.

The average crystallite size and microstrain of the YSZ phase were calculated from XRD data and reported in Table 1. For both viscosity values, samples with lower organic concentration (lower R) showed lower crystallite size, because the peaks are broader than those with $R=3$ and 5, besides presenting higher microstrain values. As shown in Table 1, for $R=1$ and $R=3$, the crystallite size increased and microstrain decreased when the sol viscosity increased, while the opposite was observed for the highest R value ($R=5$). It is concluded that high organic concentration favors the crystallite growth during sintering.

Table 1 Crystallite size and microstrain of YSZ films deposited on LSM substrates for two viscosities (60 mPa·s and 100 mPa·s) and three R values (1, 3 and 5)

$R=C_o/C_s$	Viscosity (mPa·s)	Crystallite size (nm)	Microstrain (%)
1	60	16.1	0.60
3	60	22.7	0.46
5	60	25.5	0.37
1	100	17.0	0.56
3	100	24.6	0.42
5	100	21.9	0.47

3.4 Morphology and microstructure of the YSZ films

Figures 5 and 6 show the surface and cross-section morphology of YSZ films deposited on LSM substrate using sol viscosity of 60 mPa·s and 100 mPa·s, respectively.

For both sol viscosity values, the surface morphology of the YSZ films is similar; however, grains of the samples with lower sol viscosity are smaller than those with higher sol viscosity. Some pinholes can be observed in the samples prepared with 60 mPa·s of sol viscosity. The cross-section micrographs indicate that the coating surface is relatively rough and the YSZ film's porosity decreases with R values increasing.

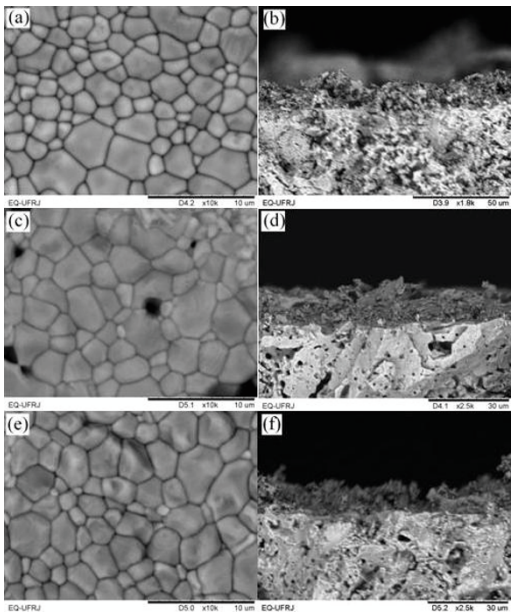

Fig. 5 SEM images of the surfaces (a), (c) and (e), and cross sections (b), (d) and (f) of YSZ films on LSM substrates with sol viscosity = 60 mPa·s and three $R=C_o/C_s$ values: (a) and (b) $R=1$; (c) and (d) $R=3$; (e) and (f) $R=5$.

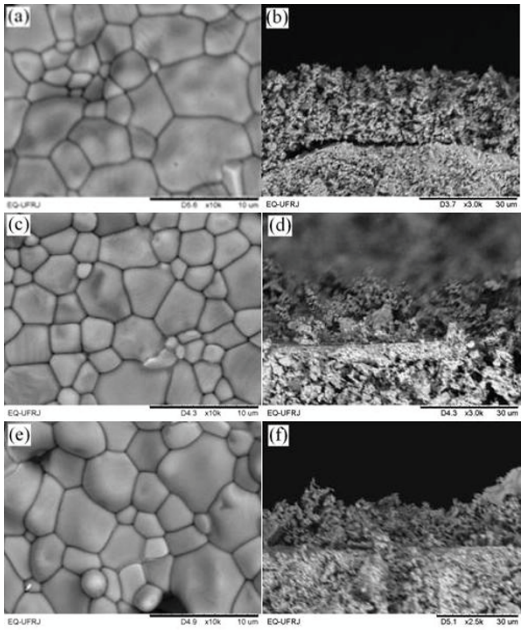

Fig. 6 SEM images of the surfaces (a), (c) and (e), and cross sections (b), (d) and (f) of YSZ films on LSM substrates with sol viscosity = 100 mPa·s and three $R=C_o/C_s$ values: (a) and (b) $R=1$; (c) and (d) $R=3$; (e) and (f) $R=5$.

For $R=1$, cross-section images show that the films are not homogeneous, with porous structure and adherence problems. The microstructure is improved

for $R = 3$, with films better adhered to the substrate, but microcracks and micropores can be observed. Nevertheless, for $R = 5$, the films appear crack-free, homogeneous and well adhered to the cathode-supported substrate. Thus, comparing the surface and cross-section morphology of the samples, it can be concluded that film prepared with $R = 5$ and sol viscosity = 100 mPa·s is more suitable for SOFC electrolyte application, although an improvement in the film density is necessary.

Table 2 shows the thickness of the YSZ films. Several authors have obtained similar values of YSZ film thickness. Yang *et al*. [2] have reported a thickness of the YSZ film deposited on the $La_{0.8}Sr_{0.2}MnO_3$ substrate using EPD method was about 16 μm. Wang *et al*. [8] have reported the preparation of YSZ thin films on NiO–YSZ anode substrate by dip-coating with different numbers of layers. The film thickness of one-layer sample was about 10 μm, of two-layer sample was 16 μm, and that of three-layer sample was 21 μm. Lenormand *et al*. [9] have investigated YSZ films on porous NiO–YSZ substrates using dip-coating process, obtaining continuous, homogeneous and 15 μm thick films. Mauvy *et al*. [21] have deposited 25 μm thick YSZ films on dense alumina substrates by sol–gel/dip-coating process. Tikkanen *et al*. [22] have obtained YSZ films with thickness of 15 μm by single-step dip-coating on NiO–YSZ substrate. Zhang *et al*. [23] have deposited YSZ films with 20–30 μm of thickness by dip-coating on NiO–YSZ supports. In general, YSZ films of 5–20 μm are suitable for application as SOFC electrolyte [3].

The film thickness increases with the sol viscosity, as shown in Table 2. According to Yoon *et al*. [24], the film thickness can be related to the sol viscosity by Eq. (2):

$$t = k(\eta\upsilon/\rho g)^{1/2} \quad (2)$$

where t is the film thickness, k a constant, η the viscosity of the solution, υ the withdrawal speed, ρ the solution density, and g is the gravitational acceleration. Similar behavior was obtained by Lenormand *et al*. [11] for $La_{0.8}Sr_{0.2}Mn_{0.8}Fe_{0.2}O_{3+\delta}$ films on YSZ substrate and Fontaine *et al*. [25] for $La_2NiO_{4+\delta}$ films on YSZ substrate. The film thickness decreased with the R value, in accordance with Lenormand *et al*. [11].

Table 2 Film thickness of the samples for both sol viscosities and three *R* values

$R = C_o/C_s$	Viscosity (mPa·s)	Thickness (μm)
1	60	15.3
3	60	14.2
5	60	11.6
1	100	23.8
3	100	19.3
5	100	18.7

Figure 7 shows the SEM micrograph of the cross section of YSZ film deposited on LSM substrate with sol viscosity = 100 mPa·s and $R = 5$, and the EDS spectra of the LSM substrate (Region 3), YSZ film (Region 1) and the YSZ/LSM interface (Region 2). The EDS analysis shows the peaks of La, Sr and Mn (correspondent to LSM substrate) and peaks of Zr (correspondent to YSZ film). The peaks corresponding to Al seen in EDS spectra are attributed to the sample compartment. No peaks of Y were observed due to its low concentration and small thickness of the film. Moreover, the presence of LSM components in Region

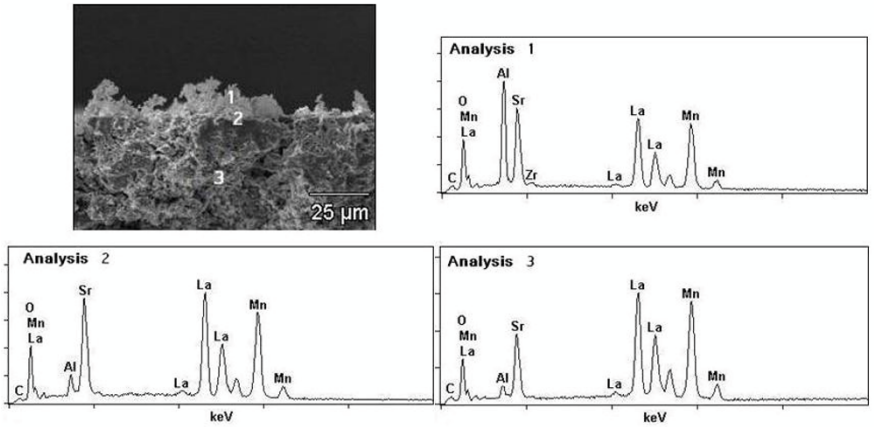

Fig. 7 SEM micrograph of the cross section of YSZ film on LSM substrate with sol viscosity = 100 mPa·s and $R = 5$ and its EDS spectra.

1 is closely related to the small thickness of the film.

Table 3 shows the weight percent of La, Sr and Mn for each analysis. The composition of Region 3 is very close to the nominal composition of LSM substrate. EDS analysis indicated a significant Sr enrichment at the electrolyte surface, which contributes to the formation of $SrZrO_3$ phase, as identified by XRD profiles (Fig. 4).

Table 3 Weight percent of La, Sr and Mn obtained from EDS (Fig. 7)

		Region 1	Region 2	Region 3
Weight%	La	33	45	49
	Sr	14	15	11
	Mn	17	22	26

According to Backhaus-Ricoult [26], there is a substantial interdiffusion across the LSM–YSZ interface with the formation of highly doped zirconia. The diffusion coefficients of ions at the LSM–YSZ interface follow the order: $D_{Sr} \ll D_{La} < D_{Mn}$. Yang *et al*. [2] observed that cations in LSM, mainly Mn and La ions, diffuse greatly into YSZ film; Zr and Y ions also diffuse into LSM, but Sr ions diffuse only slightly into YSZ. These authors only observed formation of LZ at the LSM–YSZ interface. In our case, it seems that Sr diffuses faster than La and Mn, favoring formation of SZ instead of LZ. More detailed studies of the interface using transmission electron microscopy (TEM) are being carried out to clarify the LSM/YSZ reactivity.

4 Conclusions

The influence of organic/metal salt concentration ratio ($R = C_o/C_s$) and sol viscosity was investigated on the deposition of YSZ films on LSM substrates. These are key parameters to obtain films with good phase formation and adequate microstructure in sol–gel/dip-coating route. LSM, cubic YSZ, $SrZrO_3$ and La_2O_3 phases were obtained. The increase in sol viscosity decreased the formation of the secondary phases. Samples with lower organic concentration showed lower crystallite size and higher microstrain. Films deposited with $R = 5$ and sol viscosity = 100 mPa·s were homogeneous, crack-free and well adhered to the substrate. The film thickness varied in the range of 11–24 μm. These synthesis parameters can be used to prepare YSZ electrolytes for cathode-supported SOFCs.

Acknowledgements

The authors thank CAPES for financial support to carry out this work.

References

[1] Yamamoto O. Solid oxide fuel cells: Fundamental aspects and prospects. *Electrochim Acta* 2000, **45**: 2423–2435.

[2] Yang K, Shen JH, Yang KY, *et al*. Characterization of the yttria-stabilized zirconia thin film electrophoretic deposited on $La_{0.8}Sr_{0.2}MnO_3$ substrate. *J Alloys Compd* 2007, **436**: 351–357.

[3] Singhal SC, Kendall K, Eds. *High Temperature Solid Oxide Fuel Cells*: *Fundamentals*, *Design and Applications*. New York: Elsevier, 2003.

[4] Jiang SP, Li J. In: *Solid Oxide Fuel Cells*: *Materials*, *Properties and Performance*. Fergus JW, Hui R, Li XG, *et al*. Eds. Boca Raton: CRC Press, 2008.

[5] Lee YH, Kuo CW, Shih CJ, *et al*. Characterization on the electrophoretic deposition of the 8 mol% yttria-stabilized zirconia nanocrystallites prepared by a sol–gel process. *Mat Sci Eng A* 2007, **445–446**: 347–354.

[6] Gaudon M, Laberty-Robert C, Ansart F, *et al*. Preparation and characterization of $La_{1-x}Sr_xMnO_{3+\delta}$ ($0 \leqslant x \leqslant 0.6$) powder by sol–gel processing. *Solid State Sci* 2002, **4**: 125–133.

[7] Gaudon M, Laberty-Robert C, Ansart F, *et al*. Evaluation of sol–gel process for the synthesis of $La_{1-x}Sr_xMnO_{3+\delta}$ cathodic multilayers for solid oxide fuel cells. *J Power Sources* 2004, **133**: 214–222.

[8] Wang ZH, Sun KN, Shen SY, *et al*. Preparation of YSZ thin films for intermediate temperature solid oxide fuel cells by dip-coating method. *J Membrane Sci* 2008, **320**: 500–504.

[9] Lenormand P, Caravaca D, Laberty-Robert C, *et al*. Thick films of YSZ electrolytes by dip-coating process. *J Eur Ceram Soc* 2005, **25**: 2643–2646.

[10] Gaudon M, Laberty-Robert C, Ansart F, *et al*. Thick YSZ films prepared via a modified sol–gel route: Thickness control (8–80 μm). *J Eur Ceram Soc* 2006,

26: 3153–3160.

[11] Lenormand P, Castillo S, Gonzalez JR, *et al*. Lanthanum ferromanganites thin films by sol–gel process. Influence of the organic/inorganic *R* ratio on the microstructural properties. *Solid State Sci* 2005, **7**: 159–163.

[12] da Conceição L, Ribeiro NFP, Furtado JGM, *et al*. Effect of propellant on the combustion synthesized Sr-doped $LaMnO_3$ powders. *Ceram Int* 2009, **35**: 1683–1687.

[13] Williamson GK, Hall WH. X-ray line broadening from filed aluminum and wolfram. *Acta Metall* 1953, **1**: 22–31.

[14] Pan Y, Zhu JH, Hu MZ, *et al*. Processing of YSZ thin films on dense and porous substrates. *Surf Coat Technol* 2005, **200**: 1242–1247.

[15] Lim DP, Lim DS, Oh JS, *et al*. Influence of post-treatments on the contact resistance of plasma-sprayed $La_{0.8}Sr_{0.2}MnO_3$ coating on SOFC metallic interconnector. *Surf Coat Technol* 2005, **200**: 1248–1251.

[16] Im J, Park I, Shin D. Electrochemical properties of nanostructured lanthanum strontium manganite cathode fabricated by electrostatic spray deposition. *Solid State Ionics* 2011, **192**: 448–452.

[17] Stochniol G, Syskakis E, Naoumidis A. Chemical compatibility between strontium-doped lanthanum manganite and yttria-stabilized zirconia. *J Am Ceram Soc* 1995, **78**: 929–932.

[18] Liu YL, Hagen A, Barfod R, *et al*. Microstructural studies on degradation of interface between LSM–YSZ cathode and YSZ electrolyte in SOFCs. *Solid State Ionics* 2009, **180**: 1298–1304.

[19] Brant MC, Matencio T, Dessemond L, *et al*. Electrical degradation of porous and dense LSM/YSZ interface. *Solid State Ionics* 2006, **177**: 915–921.

[20] van Roosmalen JAM, Cordfunke EHP. Chemical reactivity and interdiffusion of (La, Sr)MnO_3 and (Zr, Y)O_2, solid oxide fuel cell cathode and electrolyte materials. *Solid State Ionics* 1992, **52**: 303–312.

[21] Mauvy F, Lenormand P, Lalanne C, *et al*. Electrochemical characterization of YSZ thick films deposited by dip-coating process. *J Power Sources* 2007, **171**: 783–788.

[22] Tikkanen H, Suciu C, Wærnhus I, *et al*. Examination of the co-sintering process of thin 8YSZ films obtained by dip-coating on in-house produced NiO–YSZ. *J Eur Ceram Soc* 2011, **31**: 1733–1739.

[23] Zhang YL, Gao JF, Peng DK, *et al*. Dip-coating thin yttria-stabilized zirconia films for solid oxide fuel cell applications. *Ceram Int* 2004, **30**: 1049–1053.

[24] Yoon JS, Lee J, Hwang HJ, *et al*. Lanthanum oxide-coated stainless steel for bipolar plates in solid oxide fuel cells (SOFCs). *J Power Sources* 2008, **181**: 281–286.

[25] Fontaine ML, Laberty-Robert C, Ansart F, *et al*. Elaboration and characterization of $La_2NiO_{4+\delta}$ powders and thin films via a modified sol–gel process. *J Solid State Chem* 2004, **177**: 1471–1479.

[26] Backhaus-Ricoult M. Interface chemistry in LSM–YSZ composite SOFC cathodes. *Solid State Ionics* 2006, **177**: 2195–2200.